frontiers in Environmental Science

ORIGINAL RESEARCH
published: 20 August 2020
doi: 10.3389/fenvs.2020.00139

Trace Metal Dynamics in a Tropical Mangrove Tidal Creek: Influence of Porewater Seepage (Can Gio, Vietnam)

Nguyen Thanh-Nho[1,2], Cyril Marchand[2,3], Emilie Strady[4,5], Truong Van Vinh[2,6], Pierre Taillardat[7], Nguyen Cong-Hau[1] and Tran-Thi Nhu-Trang[1]*

[1] Faculty of Environmental and Food Engineering, Nguyen Tat Thanh University, Ho Chi Minh City, Vietnam, [2] IMPMC, Institut de Recherche pour le Développement (IRD), UPMC, CNRS, MNHN, Noumea, France, [3] ISEA, Université de la Nouvelle-Calédonie (UNC), Noumea, France, [4] Aix-Marseille Univ., Mediterranean Institute of Oceanography (MIO), Marseille, Université de Toulon, CNRS/IRD, France, [5] CARE-HCMUT, Ho Chi Minh City, Vietnam, [6] Department of Forest Resources Management, Faculty of Forestry, Nong Lam University HCMC, Ho Chi Minh City, Vietnam, [7] GEOTOP, Université du Québec à Montréal, Montréal, QC, Canada

OPEN ACCESS

Edited by:
Gaetane Lespes, Université de Pau et des Pays de l'Adour, France

Reviewed by:
Xueyan Jiang, Ocean University of China, China
Nadia Valentina Martínez-Villegas, Instituto Potosino de Investigación Científica y Tecnológica (IPICYT), Mexico

***Correspondence:**
Cyril Marchand
cyril.marchand@unc.nc

Specialty section:
This article was submitted to Biogeochemical Dynamics, a section of the journal Frontiers in Environmental Science

Received: *20 February 2020*
Accepted: *23 July 2020*
Published: *20 August 2020*

Citation:
Thanh-Nho N, Marchand C, Strady E, Van Vinh T, Taillardat P, Cong-Hau N and Nhu-Trang T-T (2020) Trace Metal Dynamics in a Tropical Mangrove Tidal Creek: Influence of Porewater Seepage (Can Gio, Vietnam). Front. Environ. Sci. 8:139. doi: 10.3389/fenvs.2020.00139

Mangrove soils are considered as sinks for trace metals, protecting coastal waters from pollutions. However, the cycling of trace metals in mangroves is complex due to various biogeochemical processes across the intertidal zone, notably the dissolution of bearing phases resulting in high trace metal concentrations in porewaters. Previous studies demonstrated a decrease of trace metal stocks in mangrove soils seaward, possibly due to the export of dissolved metals through tidal pumping. Can Gio mangrove is the largest one in Vietnam, developing downstream Ho Chi Minh City (Viet Nam's biggest industrial city). The objectives of the present study were to characterize the dynamics of trace metals in a tidal creek of the Can Gio mangrove that does not receive any upstream inputs and to identify the role of porewater seepage on their dynamics. To reach our goals, surface water and suspended particulate matters were collected every 2 h during two different tidal cycles (spring and neap tides) and at the two different seasons, dry and wet. Mangroves porewaters were also collected. In addition to particulate and dissolved trace metals, physico-chemical parameters and a groundwater tracer (Radon – ^{222}Rn) were measured. The results showed that trace metal concentrations at flood tides, both in the dissolved and the particulate phases, were in the same range that those measured in the Can Gio Estuary. Then during ebb tides, we evidenced high inputs of dissolved Fe, Mn, Co, and Ni from mangrove soils. However, the dynamics of these inputs differed depending on the element considered. Mn was exported from the tidal creek in its dissolved form. However concerning Fe, and to a lesser extent Co and Ni, we suggest that, when delivered to the creek from the soils under dissolved forms, these trace metals precipitated because of different physicochemical characteristics between mangrove soils and tidal creek, notably higher

dissolved oxygen concentrations and higher pH. Consequently, these elements were exported to the estuary in particulate forms. We suggest that budget studies of trace metals in mangroves should be developed like the ones concerning carbon to efficiently determine their role as a barrier for pollutants between land and sea.

Keywords: mangrove, trace metals, tidal creek, partitioning, monsoon, Vietnam

INTRODUCTION

Mangrove forests can trap suspended solids, with their load of trace metals originating from upstream soils, rocks, or anthropogenic activities (Wolanski, 1995; Furukawa et al., 1997; Tam and Wong, 1999). Mangroves are, thus, considered as efficient barriers between land and sea, being sinks for trace metals and protecting coastal waters from pollutions. However, this ability may depend on soil characteristics and hydrology (Kaly et al., 1997). Trace metals dynamics in mangroves are complex due to various biogeochemical processes across the intertidal zone (McKee, 1993; Marchand et al., 2011; Noël et al., 2015). Numerous physicochemical parameters, such as redox, pH, sulfides, and salinity, can influence the distribution of trace metals between solid and liquid phases in mangrove soils, and thus their transfer at the soil-water interface (Patrick and Jugsujinda, 1992; Van Ryssen et al., 1998). Because of metal toxicities to mangrove biodiversity and also to human health, their cycling is a serious question addressed by many authors during the last few decades (Lacerda et al., 1988; Clark et al., 1998; Ferreira et al., 2007) and recently (Xiao et al., 2015; Marchand et al., 2016). In most of the published studies, authors focused on trace metal distributions and dynamics between soils, porewaters, and plants. Only a few and recent publications were interested in the transfer of trace metals from mangrove soils to tidal creeks through tidal pumping and porewaters seepage (Sanders et al., 2015; Holloway et al., 2016). Tidal pumping induces advective flushing of permeable soils and the transport of organic and inorganic products to the open water column (Maher et al., 2013). Other recent studies measured a decrease of the stocks of some trace metals in mangrove soils from the landside to the seaside of the studied forests due to a more reactive substrate that leads to the enhanced dissolution of metals bearing phases (Noël et al., 2014; Deborde et al., 2015; Marchand et al., 2016). In previous studies concerning trace metals distribution in Can Gio mangrove (Thanh-Nho et al., 2019a,b), we showed that trace metals dynamics in the soil as well as their transfer to mangrove plants were notably driven by the position of the stand and the soil organic matter content. We also demonstrated that trace metal stocks were lower in the mangrove soils than in the mudflat, and that concentrations in mangrove porewaters could be really high. Consequently, we suggested that the export of dissolved trace metals through tidal pumping may occur.

In the present study, we were interested in trace metal dynamics in a mangrove tidal creek of the Can Gio mangrove adjacent to the forest we previously studied. This tidal creek is 1,400 m long and do not receive any upstream inputs. Our objectives were to understand the variability of trace metals (Fe, Mn, Co, Ni) concentrations and distributions between the particulate and the dissolved phases with tides and seasons, and thus to confirm our hypothesis of export of trace metal from mangrove soils to tidal creeks. We were also interested in the relationships between physicochemical parameters [pH, salinity, dissolved oxygen (DO), dissolved organic carbon (DOC), particulate organic carbon (POC), total suspended solids (TSS)] and trace metals. Our main hypothesis was that dissolved metal concentrations in the tidal creek would increase during the ebb tide as a result of inputs from mangrove soils. To reach our goals, we collected waters and suspended matters every 2 h during 24 h at different tidal cycles and at distinct seasons (dry and rainy). Physico-chemical parameters of the water column were monitored continuously during the sampling. Groundwater tracer (Radon – ^{222}Rn) in the water column and dissolved metal concentrations in porewaters were also measured.

MATERIALS AND METHODS

Study Site

The studied tidal creek is situated in the core zone of the Can Gio mangrove (10°30.399N-106°52.943E), and has approximately 1,400 m of length (**Figure 1**). This tidal creek does not receive any direct freshwater inputs except for rainwater. The Can Gio mangrove (i.e., 35,000 ha) accounts for 20% of the total mangrove area in Vietnam and is located downstream Ho Chi Minh City (Vietnam's biggest industrial city). It is considered as one of the most beautiful mangroves of Southeast Asia, and is usually classified as "Mangrove afforestation and re-forestation area" (Blasco et al., 2001), and has been declared as a World's Biosphere Reserve by the UNESCO since 2000. The tidal regime is irregular semi-diurnal. The climate is typical of the monsoonal zone with two distinct seasons, in which the dry season starts in November and lasts until the end of May, the wet season starts from the end of May until the end of October. The annual mean precipitation is ∼1,400 mm, with ∼90% of the precipitation falling during the wet season. The annual mean temperature ranges from 26.5 to 30°C. The Can Gio mangrove has a high biodiversity with more than 200 species of fauna and 52 species of flora. The dominant mangrove species are *Rhizophora apiculata* and *Avicennia alba* (Luong et al., 2015). The main economic activities of the local people in the Can Gio mangrove are aquacultures, fishing, and salt production (Kuenzer and Tuan, 2013).

Field Sampling

For each sampling period, during the dry season (April 11th – 12th and 18th – 19th, 2015) and the wet season (October 19th – 20th and 26th – 27th, 2015), a boat was anchored in

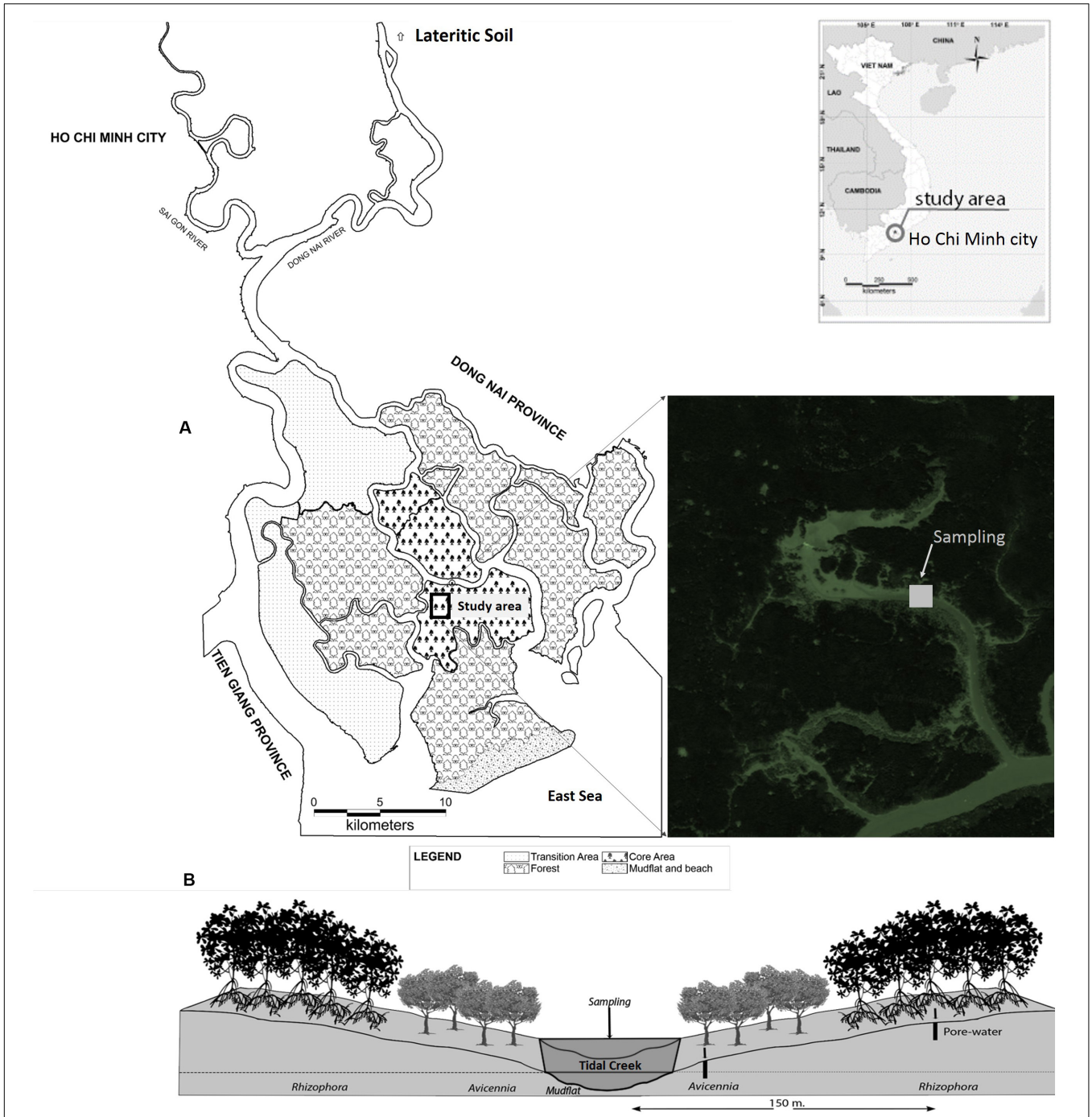

FIGURE 1 | Map of the study area showing: **(A)** the location of Can Gio mangrove in Vietnam and the location of the study site in Can Gio; and **(B)** the cross-section of the tidal creek without any direct fresh-water inputs except from rainwater.

the middle of the tidal creek (**Figure 1**). For each season, two series of the 24 h (24-h) were carried out during asymmetric and symmetric tidal cycles. During each sampling campaign, surface waters (50 cm below the water-air interface) were collected in duplicates every 2 h using a pre-decontaminated bucket. The water samples were immediately transferred into acid pre-cleaned polypropylene bottles (1 L) – previously rinsed with estuarine water. After that, these samples were filtered through 0.2 μm JG PTFE Omnipore^{TM} Membrane Filters: the filtrates were then transferred into pre-cleaned 50 mL polypropylene tubes, immediately acidified to pH <2 using concentrated suprapur® HNO_3 (HNO_3: sample = 1:1000 (v/v)) for sample preservation until trace metals analysis (Strady et al., 2009). The filters were stored in small plastic boxes with closed cover

for future analyses of trace metals concentrations in suspended particulate matters. Both types of samples were stored in a cooler box during the sampling campaign and then stored at 4°C at the laboratory until analysis. Filtration for the determination of TSS, POC, and DOC was also simultaneously carried out as follow: (i) water samples were filtered through pre-combusted and pre-weighted glass fiber filters (Whatman® GF/F 0.7 μm); (ii) the filters were stored at −20°C, and the filtrates were transferred into sterile 15 mL polypropylene tubes; (iii) these filtrates were then acidified using concentrated suprapur® HCl and stored at 4°C until DOC analysis (Thanh-Nho et al., 2018).

Mangrove porewaters were also collected along a transect from the tidal creek to the upper intertidal area. One hole beneath each mangrove stand (i.e., *R. apiculata*, *A. alba*) and in the mudflat were drilled to approximately 1 m depth at low tide, using an Eijkelkamp gouge auger. The holes were purged at least two times with a hand pump before sampling. All samples were filtered through 0.45 μm Sartorius® filter, stored in pre-cleaned 50 mL polypropylene, and were then acidified to pH <2 using concentrated suprapur® HNO_3 (Merck), and stored at 4°C until analysis.

In situ Measurements of Physicochemical Parameters

Surface water salinity and pH were logged continuously using a multi-probe (Yellow Spring Instrument® meters YSI 6920). The pH probe was calibrated using buffer solutions: 4, 7, and 10 (NIST scale). DO was monitored with a HOBO Dissolved Oxygen data logger (HOBO U26-001). These above probes were immerged 50 cm below the water-air interface. Data were recorded every 5 min. Water level profiles were measured using a Hondex PS-7.

Radon is considered as a natural groundwater tracer, widely used to quantify porewater exchange in a mangrove system (Maher et al., 2013; Tait et al., 2016; Taillardat et al., 2018a). ^{222}Rn measurements were performed only during the wet season because of a system failure during the dry one. ^{222}Rn concentrations in creek waters were measured using a showerhead equilibrator. The head-space gas was streamed into an automated ^{222}Rn-in-air analyzer with the Rad Aqua package installed (RAD 7, Durridge Co.) (Burnett et al., 2001). The ^{222}Rn monitor logged data at 30 min intervals, resulting in analytical uncertainty <10% for individual concentrations, except during the first 3 h when the analytical uncertainty was 30%.

Three soil cores (1 m depth) beneath *R. apiculata*, *A. alba*, and in the mudflat were collected using an Eijkelkamp gouge auger for *in situ* measurements of pH and salinity. For each parameter, the value was recorded every 10 cm. pH was measured using a glass electrode (pH 3110-WTW), which was calibrated using standard buffer solution of 4, 7, and 10 (NIST scale). Salinities were determined using an ATAGO refractometer (S-10, Japan) after extracting a drop of porewater from each soil layer.

Sample Analysis

Dissolved Metal (M_D) Concentrations

Mn_D, Co_D, and Ni_D concentrations in the filtrates were analyzed after matrix separation (notably dissolved solids and chloride ions) and pre-concentration by solid-liquid extraction, using 6 mL *DigiSEP* Blue® cartridges (SCP SCIENCE), with amino–diacetate as a functional group. The experimental steps are described in Strady et al. (2009). Fe_D concentrations in the filtrates were analyzed after two-folds dilution with deionized water. Dissolved trace metal concentrations were then, measured by ICP-MS (Agilent 7700×) using spike ^{103}Rh and ^{197}Au as internal standards. The analytical precision and accuracy were evaluated using certified reference material of estuarine water (SLEW-3, **Table 1a**). All reagents were suprapur grade (Merck).

Particulate Metal (M_P) Concentrations

Particulate Fe, Mn, Co, and Ni concentrations were quantified according to total extractable metal digestion adapted from the USEPA 3051a method (USEPA, 2007). The experimental steps and analytical evaluations are described in Thanh-Nho et al. (2018). In brief, a mixture of 6 mL concentrated HNO_3 and 2 mL of concentrated HCl was used for sample preparation. Co_P and Ni_P concentrations were analyzed by ICP-MS (Agilent 7700×) using ^{103}Rh and ^{197}Au as internal standards. Fe_P and Mn_P concentrations were measured using Flame Atomic Absorption Spectrophotometer (Shimadzu AA-6650). The analytical precision and accuracy were insured by analyzing certified reference material of estuarine sediments (BCR-277R), which were also intercalated in each batch of samples digestion (**Table 1b**).

Dissolved Organic Carbon (DOC) and Particulate Organic Carbon (POC)

Dissolved organic carbon was measured using a Shimadzu® TOC-L series analyzer employing a 680°C combustion catalytic oxidation method. The analyzer was coupled to a solid sample module (SSM-5000A) heated up to 900°C for the POC determinations (Leopold et al., 2013). A 40% glucose standard was used for calibrations. Repeated measurements of different standards concentrations indicated deviations <2%.

Data Calculations

The partitioning coefficient (K_D) was calculated to get a better understanding of the interaction of trace metals between dissolved and particulate phases during tidal cycles. K_D is defined as the ratio of particulate metal concentration (M_P) to dissolved metal concentration (M_D) in the water column (Turner et al., 1993).

$$K_D = M_P / M_D$$

where, M_P is a particulate metal concentration and M_D is a dissolved metal concentration.

Pearson correlation coefficients was determined using the statistical package for the social science software (SPSS: version 23) to identify major relationships between metal concentrations and the physicochemical parameters as well as interrelationships between metal concentrations together, which help to clarify the main factors controlling metal partitioning between particulate and dissolved phases.

TABLE 1 | Quality control of analytical methods applied for dissolved and particulate metal concentration analysis including accuracy, precision, and quantitation limit, using: (a) estuarine water SLEW-3; (b) sediment BCR-277R.

(a) Dissolved metal concentration analysis

Element	Quantitation limit ($\mu g\ L^{-1}$)	Certified values ($\mu g\ L^{-1}$)	Measured values ($\mu g\ L^{-1}$)	Recovery (%)	Relative standard deviation (%)
Fe	0.20	0.568 ± 0.059	0.682 ± 0.068	120	10
Mn	0.09	1.61 ± 0.22	1.48 ± 0.10	92	7
Co	0.05	0.042 ± 0.010	0.0464 ± 0.0025	116	15
Ni	0.11	1.23 ± 0.07	1.37 ± 0.11	112	8

(b) Particulate metal concentration analysis

Element	Certified values ($mg\ kg^{-1}$)	Measured values ($mg\ kg^{-1}$, n = 9)	Recovery (%)	Relative standard deviation (%)	Analytical method
Fe	NA	51855 ± 3146	–	6.1	FAAS
Mn	NA	835 ± 29	–	3.5	FAAS
Co	22.5 ± 1.4	22.9 ± 0.7	102	2.8	ICP-MS
Ni	130 ± 8	128.9 ± 3.2	99	2.5	ICP-MS

RESULTS

Physico-Chemical Parameter Variability

The temporal variations of water levels, salinity, pH, DO, TSS, POC, and DOC during the four tidal cycles are presented in **Figure 2**. Salinity presented different distribution patterns between seasons, ranging from 22 to 23 and 18.5 to 22 during the dry and wet seasons, respectively. The highest salinity values were measured at the lowest water levels during the dry season, while during the wet season, the opposite trend was observed. pH values varied from 7.0 to 7.5 during the dry season and from 6.7 to 7.2 during the wet season. DO was higher during the dry season than the wet one (4.6–6.4 $mgO_2\ L^{-1}$ vs. 2.1–4.2 $mgO_2\ L^{-1}$, respectively). TSS concentrations varied between the four tidal cycles (i.e., 36–119 mg L^{-1} in neap tide vs. 60–675 mg L^{-1} in spring tide during the dry season; 54–291 mg L^{-1} vs. 60–460 mg L^{-1} in neap and spring tides during the wet season, respectively). For each tidal cycle, the highest TSS concentrations were measured at the lowest water level. POC ranged from 0.9 to 2.4% for all tidal cycles. A higher POC amplitude was observed during spring tides (1.03–2.41 and 0.8–2.37% in the dry and the wet seasons, respectively) than neap ones (1.6–1.72 and 0.9–1.6% in the dry and wet seasons, respectively). The highest POC concentrations in each tidal cycle were measured at the lowest water level. DOC values were in the same range for all tidal cycles and varied from 129.5 to 192.1 $\mu molC\ L^{-1}$. The maximum DOC values were measured at the lowest water level, whatever the tidal cycle. ^{222}Rn concentrations in the surface waters increased during the ebb and reached maximum values at the lowest water level (**Figure 2**).

Dissolved Metal (M_D) Concentrations

Fluctuations of Mn_D, Fe_D, Co_D and Ni_D concentrations during 24-h tidal cycles are presented in **Figure 3**. All trace metals presented higher mean concentrations during the wet season than during the dry season. In addition, trace metals concentrations were higher at low tides than at high tides. Mn_D increased during ebb tides and reached maximum values at the lowest water level for all tidal cycles. During the dry season, Mn_D reached 1,530 and 510 $\mu g\ L^{-1}$, respectively, whereas during the wet season, they reached 1,779 and 1,274 $\mu g\ L^{-1}$ for neap and spring tides, respectively. The same pattern was observed for Fe_D with maximum values of 194, 17, 193, and 85 $\mu g\ L^{-1}$ at lowest water levels for neap and spring tidal cycles during the dry season and the wet season, respectively. Co_D concentrations varied from less than 0.1 $\mu g\ L^{-1}$ to approximately 2.0 $\mu g\ L^{-1}$. The highest Co_D was also observed during the periods of the lowest water levels. Ni_D was under the detection limit (i.e., $<0.11\ \mu g\ L^{-1}$) during the dry season, and varied from 0.78 to 3.48 $\mu g\ L^{-1}$ during the wet season, with high values also observed at low tides.

Particulate Metal (M_P) Concentrations

Variability of Mn_P, Fe_P, Co_P, and Ni_P concentrations during 24-h tidal cycles are shown in **Figure 4**. Mn_P and Fe_P mean concentrations did not differ between seasons, however and like the dissolved concentrations, they were strongly influenced by tides but differently. Mn_P concentrations ranged from 320 to 1,024 mg kg^{-1}, decreasing during the ebb. Fe_P concentrations ranged from 34,000 to 50,000 mg kg^{-1}, but conversely to Mn, the highest values were measured at the lowest water levels. Co_P concentrations varied with seasons, ranging from 5.7 to 11.7 mg kg^{-1} during the dry season, and from 9.1 to 19.8 mg kg^{-1} during the wet season. Ni_P concentrations were quite stable with tides, showing higher concentrations during the wet season than during the dry season, with mean concentrations of 42 and 30.7 mg kg^{-1}, respectively.

Porewater Characteristics

Salinity and pH values, as well as the average concentrations of trace metals (Fe, Mn, Co, and Ni) in mangrove porewaters during the two seasons, are presented in **Table 2**. We calculated mean values using all the samples collected in the three zones: mudflat, *A. alba*, *R. apiculata*. Salinity varied from 20 to 28 during the dry season and 14 to 22 during the rainy season. pH

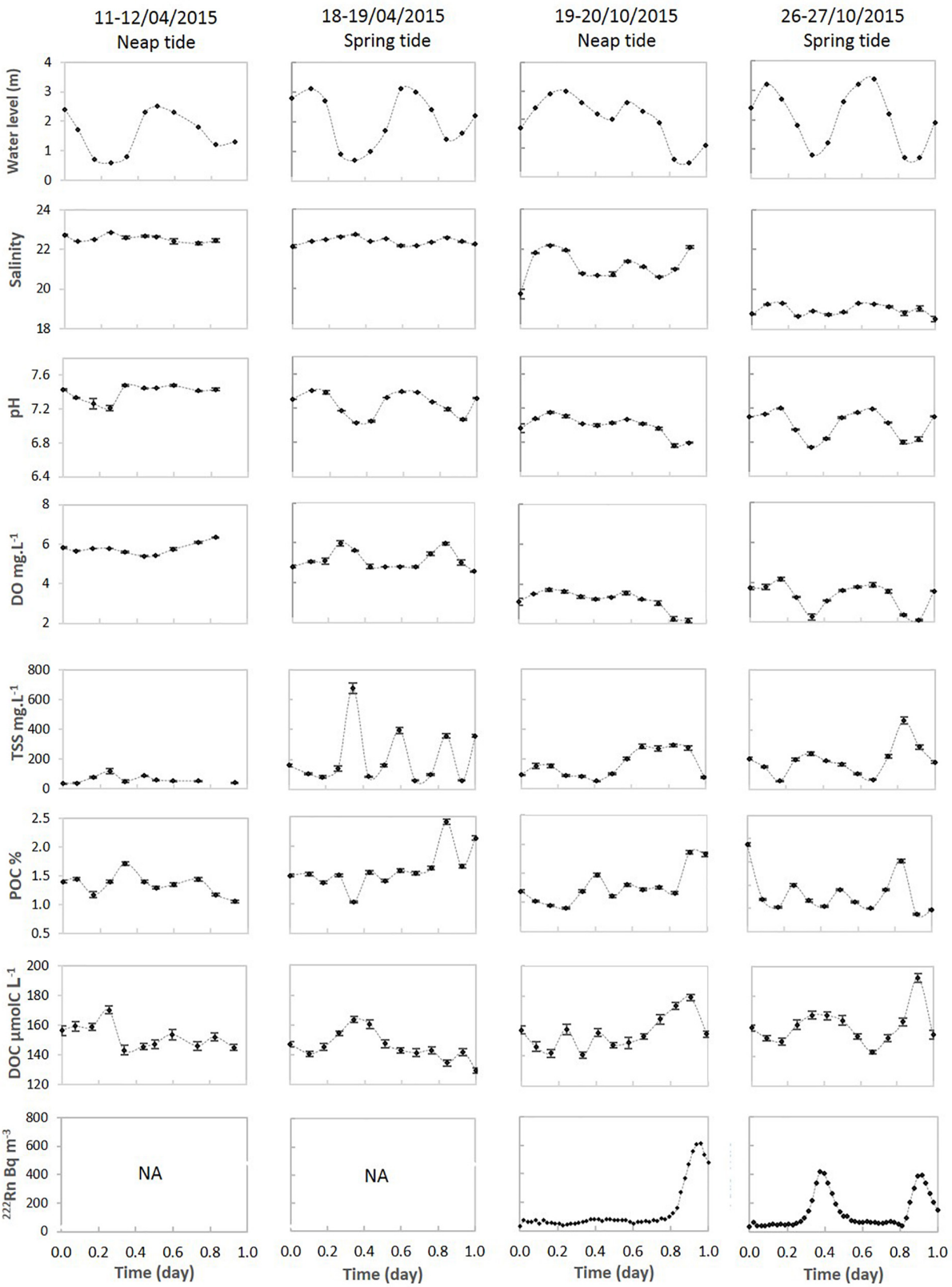

FIGURE 2 | Temporal variations of water level, salinity, pH, DO, TSS, POC, and DOC measured during neap and spring tidal cycles during the dry season (04/2015) and the wet season (10/2015). NA: not available.

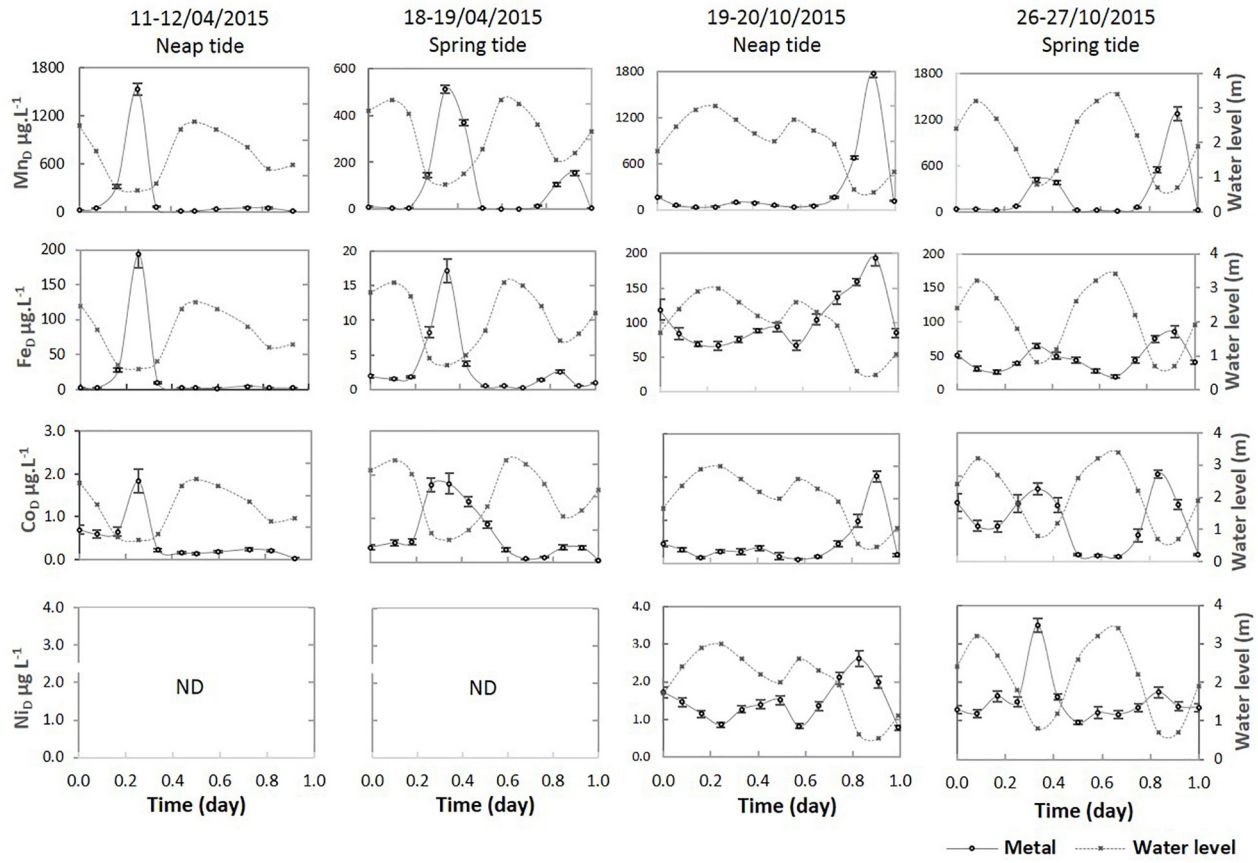

FIGURE 3 | Temporal fluctuations of dissolved metal concentrations (M_D) during the neap and the spring tidal cycles during the dry season (04/2015) and the wet season (10/2015). ND: not detection.

ranged from 4.6 to 6.7 during the dry season, and from 5.5 to 6.8 during the rainy season. Most dissolved metal concentrations presented higher amplitudes during the wet season than the dry season except for Co. Mean Fe concentrations were 1,203 ± 780 and 2,429 ± 2,744 µg L^{-1} during the dry and the wet season, respectively. Mean Mn concentrations were 1,523 ± 919 µg L^{-1} during the dry season and 2,891 ± 1,768 µg L^{-1} during the wet season. Co and Ni concentrations were far lower than Fe and Mn ones, being 9.4 ± 8.5 and 5.7 ± 0.9 µg L^{-1} for Co and 1.2 ± 0.8 and 9.0 ± 8.7 µg L^{-1} for Ni during the dry and the wet seasons, respectively.

DISCUSSION

Temporal Variability of Mangrove Tidal Creek Characteristics

In Can Gio, mangrove porewaters in the different stands studied were acidic and enriched in DOC, which is consistent with previous studies that showed that because of the high productivity of mangrove forests, DOC concentrations in porewaters could be really high (Marchand et al., 2006; Sadat-Noori and Glamore, 2019), and that because of organic matter decomposition (Taillardat et al., 2018b) and possible sulfide oxidation (Marchand et al., 2012), mangrove soils are usually acidic. The observed correlations between pH, DOC and water level in the tidal creek whatever the season (**Tables 3**, **4** and **Supplementary Figure S1**) provide evidences that porewater inputs partly controlled tidal creek characteristics. This was confirmed by the ^{222}Rn concentrations evolution with tides, even though other parameters such as estuarine waters inflow during the flood and *in situ* biogeochemical processes may be involved. The key role of mangrove porewater seepage on tidal creeks was recently evidenced in several studies (Bouillon et al., 2008; Call et al., 2015; Dittmar and Lara, 2001; Maher et al., 2013). In addition, at low tides, DOC concentrations were higher and pH values were more acidic during the rainy season than during the dry season (**Figure 2**). These results may suggest a greater contribution of mangrove porewaters to the tidal creek during the rainy season because of the larger volume of water exchanged between mangrove soils and mangrove creek, and because of a larger mangrove area immerged resulting from the higher water level. In addition, higher temperature during summer may also be involved, inducing enhanced processes of organic matter decomposition in mangrove soils as suggested in other studies (Taillardat et al., 2019; Vinh et al., 2020). Mangrove

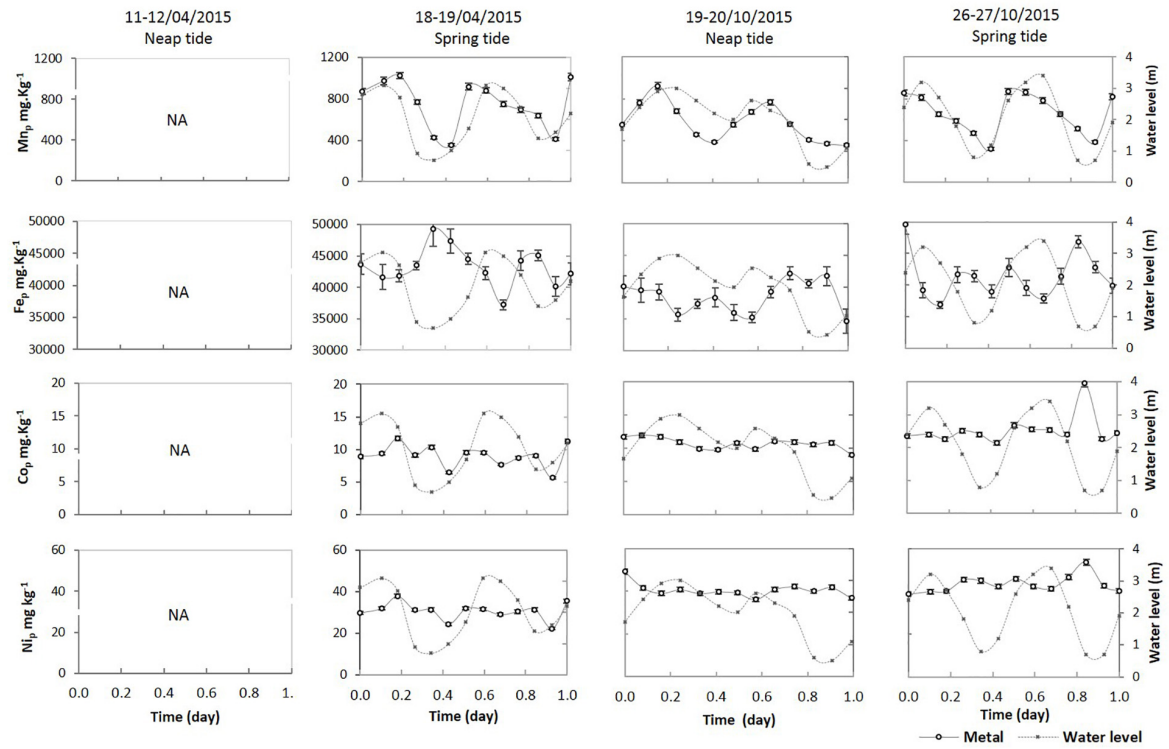

FIGURE 4 | Distributions of the particulate metal concentrations (M_P) during neap and spring tidal cycles during the dry season (04/2015) and the wet season (10/2015). NA: not available.

soils are most of the time anoxic (Kristensen et al., 2017), which is also the case for Can Gio (Thanh-Nho et al., 2019b; Vinh et al., 2019). The very low DO concentrations measured at low tide in the tidal creek, may also confirm porewater seepage. The even lower concentrations during the rainy season may also be consistent with our hypothesis of enhanced OM decomposition in mangrove soils during this season. However, the relationship with the water level in the creek was not always clear. In a previous study concerning the same tidal creek (David et al., 2018), it was suggested that algal cells could grow at low tide using nutrients and CO_2 provided by the tidal pumping of mangrove porewater, and thus resulting in increased DO content. In mangrove soils, salinity can be highly variable with depth and between mangrove stands, depending on the salinity of the incoming water (estuarine waters or rainfall) and evapotranspiration processes (Marchand et al., 2004). However in Can Gio, the low salinity differences between the estuarine waters and the porewaters, which was related to the humid tropical climate, prevent the use of salinity to trace porewater inputs to the tidal creek studied. Nevertheless, the intense rainfall occurring during the rainy season induced slightly lower salinity values during the rainy season both in the porewaters and in the tidal creek. Concerning TSS variability, we suggest that resuspension and bottom erosion can be the main drivers when the water level is low and the flow is rapid, either in the mangrove or in the creek. There were no significant differences in POC concentrations between seasons, and most of the time POC concentrations were higher at low tide. In mangrove tidal creeks, POC concentrations significantly increased due to particle resuspension, either from mangrove soils or creek bottom (Bouillon et al., 2008).

Tidal and Seasonal Dynamics of Trace Metals in the Mangrove Creek

Manganese Dynamic

The high Mn_P concentrations measured in the tidal creek during the flood periods, irrespective of the seasons, may be related to the high Mn_P concentrations measured at the mouth of the Can Gio mangrove estuary, reaching up to 800 mg kg^{-1} (Thanh-Nho et al., 2018). Consequently, in the tidal creek studied, the positive correlations between Mn_P and the water levels during the dry and the wet seasons (**Supplementary Figure S1**) suggest that Mn_P mainly originated from the estuary. However, the correlation between Mn_P and TSS was low (**Tables 3**, **4**). This result may be attributed to the fact that the fluctuation of TSS during the tidal cycles in the creek mainly depended on particle resuspension during the ebb, either from mangrove soils or creek bottom with Mn concentrations lower than those measured in the estuary (Thanh-Nho et al., 2018). Thanh-Nho et al. (2019b) showed that trace metals in the Can Gio mangrove soils have mainly a natural origin, being deposited in the mangrove as oxyhydroxides originating from the upstream lateritic soils with richness in hematite and goethite minerals (Egawa and Ooba, 1963). Therefore, we

TABLE 2 | Characteristics of mangrove sediments and porewaters.

Parameter	Dry season	Wet season	References
Fe (μg/L)	1,203 ± 780	2,429 ± 2,744	Present Study
Mn (μg/L)	1,523 ± 919	2,891 ± 1,768	
Co (μg/L)	9.4 ± 8.5	5.7 ± 0.9	
Ni (μg/L)	Na	9.0 ± 8.7	
pH	4.6–6.7	5.5–6.8	
Sal	20–28	14–22	
Eh (mV)	−107 to − 262		(Thanh-Nho et al., 2019b)
OC (%)	2.1–4.6		
Sand (%)	5.0 ± 6.7		(Taillardat et al., 2018a)
Silk (%)	87.8 ± 6.2		
Clay (%)	7.8 ± 2		
DIC (mmol m^{-3})	4,861 ± 2,398		
DOC (mmol m^{-3})	219 ± 78.6		
^{222}Rn (dpm m^{-3})	77,520 ± 41,660		

Mean concentrations (n = 3) ± SD; na: not available.

suggest that Mn_P mainly originates from the estuary and thus increases in the tidal creek when the contribution of the estuarine waters increases, and thus with the flood. Variations of Mn_D concentrations in the tidal creek were the opposite of Mn_P. In the Can Gio mangrove estuary, dissolved Mn concentrations were low, with a mean value of 1.3 μg L^{-1} (Thanh-Nho et al., 2018), which corresponds to what we measured in the creek at high tide. However, at low tide, Mn_D concentrations in the tidal creek reached up to 1,800 μg L^{-1} (**Figure 3**). Therefore, the contribution of Mn_D possibly originating from other sources is suggested. The enrichment of mangrove-derived organic matter from the mudflat to the *Rhizophora* stand was suggested to induce the reductive dissolution of Fe-Mn oxyhydroxides by bacteria for organic matter decay processes (Thanh-Nho et al., 2019b). Noël et al. (2014) showed that tidal fluctuations may be a major cause for continuous Fe reduction–oxidation cycles in mangrove wetlands. This process could release trace metals in porewaters, with Mn_D concentration reaching up to 2,891 ± 1,768 μg L^{-1} (**Table 2**). Considering the matrix of Pearson correlation coefficient between trace metals concentrations and physicochemical parameters in the creek water (**Tables 3**, **4**), we suggest that Mn_D originated from mangrove soils, and was exported through porewater seepage as observed in Australian mangroves (Holloway et al., 2016). This hypothesis is supported by positive correlations between Mn_D and ^{222}Rn. We also suggest that organomanganese complexes were possibly formed. Previous studies described the coupling between DOC and redox-sensitive elements, like Mn (Dang et al., 2015), and a positive correlation between DOC and Mn_D was measured (**Supplementary Figure S2**). In the tidal creek, Log $K_D{}^{Mn}$ varied in a larger range (i.e., from 2.32 to 5.72, **Figure 5A**) than in the Can Gio mangrove estuary [i.e., from 4.5 to 5.8 (Thanh-Nho et al., 2018)]. We suggest that the drop of Log $K_D{}^{Mn}$ observed at the low tides during both seasons in the tidal creek resulted from the increasing porewater Mn_D inputs. The positive correlation between Log $K_D{}^{Mn}$ and the water level may be related to the decrease of dissolved Mn by either the physical mixing between porewater and estuarine water containing lower Mn_D concentrations or the Mn_D adsorption onto particulate matter with pH increases during the flood. Along the salinity gradient of the estuary, Thanh-Nho et al. (2018) suggested that pH and DO increases resulted in Mn_D adsorption onto particle surface by the simultaneous oxidation and precipitation of dissolved Mn (II) to insoluble Mn (III) and Mn (IV) (hydr)oxides, as previously observed by Fang and Lin (2002). It is thus possible that pH also plays an important role in the fluctuation of Mn_D concentrations in the creek studied during the tidal cycles, supported by a negative correlation between Mn_D and pH (**Tables 3**, **4**). Additionally, we observed that the highest Mn_D concentrations were measured at the low tide of high amplitude cycle following a tidal cycle of low amplitude (**Figure 3**). We suggest that due to the low amplitude of the previous tidal cycle, Mn_D produced by Mn oxyhydroxide dissolution accumulated in mangrove soils, and was then exported during the tidal cycle of higher amplitude. Consequently, in the specific system of the Can Gio mangrove, the intensity of the export of dissolved Mn was not only related to the alternation between spring tides and neap tides, but also to the irregularity of the tidal cycles. Eventually, we measured higher Mn_D concentrations in the tidal creek during the rainy season. We suggest that these higher concentrations were related to higher Mn_D concentrations in porewaters (**Table 2**). Vinh et al. (2020) showed that during the rainy season, the elevated temperature and the high rainfall induced enhanced mineralization rates of leaf litter, which may have resulted in higher Mn_D production in mangrove soils. In addition, during the rainy season, the water level of the river and thus of the tidal creek was higher. Consequently, at high tide, mangrove immersion was more important during the rainy season, which may have induced increased exchanges between mangrove soils and tidal creek, also possibly partly explaining the higher Mn_D in the tidal creek during the rainy season. These results confirm those of Holloway et al. (2016), who showed that porewater exchange could release large amounts of dissolved Mn to mangrove creeks, and then to the nearby ocean surface water.

Iron Dynamic

In the mangrove tidal creek studied, Fe, which is a redox-sensitive element like Mn (Lacerda et al., 1999), presented the same variability than Mn in the dissolved phase but the opposite one in the particulate phase. In fact, the highest Fe_P concentrations were measured at low tide (**Figure 4**) irrespective of the season or the tidal range, reaching almost 50,000 mg kg^{-1} during the rainy season. Conversely, at high tide, Fe_P varied between ∼35,000 and 45,000 mg kg^{-1}, which was the same range as what was measured in the Can Gio mangrove estuary (Thanh-Nho et al., 2018) for a similar range of salinity than in the tidal creek. Consequently, we suggest that at high tide in the creek, Fe_P concentrations were related to the estuarine inputs and originated from the lateritic soils developing upstream like for Mn (Egawa and Ooba, 1963). In the Can Gio mangrove estuary, Fe_D concentrations were never higher than 30 μg L^{-1}, while at low tide in the tidal creek, they reached almost 200 μg L^{-1}. Consequently, like for Mn_D, another sources than the estuarine waters must be considered. In mangrove porewaters, mean Fe_D

TABLE 3 | Matrix of Pearson correlation coefficients between trace metal concentrations and different physicochemical parameters in the tidal creek during the dry season.

(a) Neap tide: 11-12/04/2015.

	MnD	FeD	CoD	NiD	Mnp	Fep	Cop	Nip	Water level	Sal	pH	DO	DOC	POC
MnD	1													
FeD	0.997**	1												
CoD	0.926**	0.918**	1											
NiD	.[b]	.[b]	.[b]	.[b]										
Mnp	.[b]	.[b]	.[b]	.[b]	.[b]									
Fep	.[b]	.[b]	.[b]	.[b]	.[b]	.[b]								
Cop	.[b]	.[b]	.[b]	.[b]	.[b]	.[b]	.[b]							
Nip	.[b]	.[b]	.[b]	.[b]	.[b]	.[b]	.[b]	.[b]						
Water level	−0.559	−0.534	−0.454	.[b]	.[b]	.[b]	.[b]	.[b]	1					
Sal	0.572	0.601	0.587	.[b]	.[b]	.[b]	.[b]	.[b]	−0.098	1				
pH	−0.786**	−0.750*	−0.848**	.[b]	.[b]	.[b]	.[b]	.[b]	0.624	−0.274	1			
DO	0.058	0.034	0.061	.[b]	.[b]	.[b]	.[b]	.[b]	−0.321	−0.439	−0.104	1		
DOC	0.766**	0.738**	0.895**	.[b]	.[b]	.[b]	.[b]	.[b]	−0.331	0.349	−0.848**	0.167	1	
POC	0.055	0.082	0.141	.[b]	.[b]	.[b]	.[b]	.[b]	0.019	0.133	0.269	−0.354	−0.073	1

(b) Spring tide: 18-19/04/2015.

	MnD	FeD	CoD	NiD	Mnp	Fep	Cop	Nip	Water level	Sal	pH	DO	DOC	POC	TSS
MnD	1														
FeD	0.821**	1													
CoD	0.779**	0.811**	1												
NiD	.[b]	.[b]	.[b]	.[b]											
Mnp	−0.804**	−0.445	−0.443	.[b]	1										
Fep	0.717**	0.671*	0.671*	.[b]	−0.432	1									
Cop	−0.228	0.201	−0.013	.[b]	0.697**	0.142	1								
Nip	−0.388	0.039	−0.133	.[b]	0.787**	−0.014	0.972**	1							
Water level	−0.791**	−0.662*	−0.781**	.[b]	0.679*	−0.680*	0.202	0.314	1						
Sal	0.571*	0.699**	0.718**	.[b]	−0.314	0.596*	0.205	0.139	−0.752**	1					
pH	−0.871**	−0.612*	−0.635*	.[b]	0.900**	−0.609*	0.469	0.599*	0.888**	−0.532	1				
DO	0.345	0.557*	0.453	.[b]	−0.311	0.375	0.052	0.053	−0.536	0.750**	−0.426	1			
DOC	0.768**	0.713**	0.870**	.[b]	−0.531	0.623*	−0.172	−0.291	−0.560*	0.460	−0.570*	0.230	1		
POC	−0.346	−0.464	−0.515	.[b]	0.102	−0.180	−0.039	0.047	0.038	−0.190	0.074	0.093	−0.756**	1	
TSS	0.474	0.650*	0.295	.[b]	−0.141	0.552	0.456	0.284	−0.321	0.346	−0.265	0.254	0.160	−0.005	1

***Correlation is significant at the 0.01 level (two-tailed). *Correlation is significant at the 0.05 level (two-tailed). b, Cannot be computed because at least one of the variables is not available.*

concentrations were 1,203 and 2,429 $\mu g\ L^{-1}$ during the dry and the rainy season, respectively (**Table 2**). As explained for Mn, Fe oxyhydroxide dissolution in suboxic conditions during organic matter (OM) diagenetic processes were responsible for these elevated concentrations (Thanh-Nho et al., 2019b), and the high temperature and intense rainfall, enhancing OM decomposition, induced the higher concentrations measured during the rainy season. Consequently, we suggest that porewater seepage was responsible for the high Fe_D concentrations measured in the tidal creek at low tide, which was even higher during the wet season because of possible increased geochemical processes in mangrove soils. This hypothesis was confirmed by the positive correlations between dissolved Fe_D concentrations and ^{222}Rn (r = 0.63, **Supplementary Figure S2**). However, the correlation was less strong than the one between Mn_D and ^{222}Rn (**Supplementary Figure S2**), which possibly suggests that Fe_D was subject to specific biogeochemical processes. In addition, Fe_D and Mn_D concentrations in mangrove soil porewaters were in the same range, but at low tide in the tidal creek, when porewater inputs were maximum, Fe_D concentrations were 10 times lower than Mn_D. However and conversely to Mn_P, Fe_P concentrations in the tidal creek were maximum at low tides, with higher values than those we measured in the estuary. Consequently, we suggest that, because of different physico-chemical properties between the tidal creek and mangrove soils, notable O_2 and pH, part of the dissolved iron that was exported from mangrove soil precipitated in the creek, explaining the high Fe_P concentrations measured at low tide and the fact that Fe_D concentrations were 10 times lower than Mn_D. In mangrove soils, pH ranged between 4.6 and 6.8 (**Table 2**), while in the tidal creek at low tide, pH was always higher than 6.5 (**Figure 2**), which can favor Fe_D precipitation even at low DO concentrations (Hatje et al., 2003).

TABLE 4 | Matrix of Pearson correlation coefficients between trace metal concentrations and different physicochemical parameters in the tidal creek during the wet season.

(a) Neap tide: 19-20/10/2015.

	MnD	FeD	CoD	NiD	Mnp	Fep	Cop	Nip	Water level	Sal	pH	DO	DOC	POC	TSS	^{222}Rn
MnD	1															
FeD	0.806**	1														
CoD	0.987**	0.846**	1													
NiD	0.537	0.830**	0.618*	1												
Mnp	−0.474	−0.480	−0.492	−0.342	1											
Fep	0.505	0.747**	0.584*	0.814**	−0.017	1										
Cop	0.014	0.198	0.074	0.301	0.653*	0.552	1									
Nip	0.150	0.540	0.249	0.449	0.021	0.594*	0.648*	1								
Water level	−0.743**	−0.829**	−0.743**	−0.638*	0.720**	−0.383	0.218	−0.152	1							
Sal	0.295	−0.201	0.239	−0.302	0.420	−0.091	0.185	−0.483	0.158	1						
pH	−0.781**	−0.900**	−0.815**	−0.868**	0.767**	−0.598*	0.195	−0.239	0.968**	0.211	1					
DO	−0.856**	−0.928**	−0.883**	−0.854**	0.707*	−0.651*	0.115	−0.244	0.976**	0.090	0.987**	1				
DOC	0.754**	0.812**	0.791**	0.608*	−0.402	0.486	0.085	0.309	−0.731**	0.118	−.778**	−0.813**	1			
POC	0.576*	0.428	0.520	0.040	−0.714**	0.026	−0.601*	−0.164	−0.682*	−0.032	−0.632*	−0.664*	0.354	1		
TSS	0.498	0.581*	0.486	0.588*	0.099	0.611*	0.229	0.022	−0.406	0.227	−0.553	−0.596*	0.612*	0.095	1	
^{222}Rn	0.732**	0.481	0.671*	0.095	−0.580*	0.062	−0.385	−0.179	−0.748**	0.383	−0.675*	−764**	0.543	0.868**	0.190	1

(b) Spring tide: 26-27/10/2015.

	MnD	FeD	CoD	NiD	Mnp	Fep	Cop	Nip	Water level	Sal	pH	DO	DOC	POC	TSS	^{222}Rn
MnD	1															
FeD	0.861**	1														
CoD	0.548	0.719**	1													
NiD	0.261	0.392	0.573*	1												
Mnp	−0.733**	−0.644*	−0.698**	−0.520	1											
Fep	0.241	0.605*	0.529	0.016	.020	1										
Cop	0.107	0.324	0.333	0.020	−0.006	0.459	1									
Nip	0.268	0.483	0.433	0.230	−0.356	0.355	0.805**	1								
Water level	−0.757**	−0.895**	−0.765**	−0.572*	0.822**	−0.384	−0.258	−0.512	1							
Sal	−0.089	−0.399	−0.327	−0.144	0.203	−0.456	−0.162	−0.208	0.563*	1						
pH	−0.716**	−0.844**	−0.791**	−0.649*	0.837**	−0.344	−0.269	−0.583*	0.938**	0.447	1					
DO	−0.852**	−0.917**	−0.717**	−0.573*	0.750**	−0.382	−0.323	−0.547	0.911**	0.353	0.944**	1				
DOC	0.819**	0.827**	0.487	0.201	−0.603*	0.438	0.001	0.239	−0.749**	−0.451	−0.753**	−.813**	1			
POC	−0.168	0.232	0.451	−0.052	0.205	0.874**	0.502	0.330	−0.090	−0.328	−0.091	−0.033	0.023	1		
TSS	0.531	0.797**	0.644*	0.254	−0.312	0.715**	0.726**	0.739**	−0.680*	−0.374	−0.643*	−0.727**	0.467	0.514	1	
^{222}Rn	0.655*	0.482	0.109	0.073	−0.618*	−0.138	−0.360	−0.127	−0.540	−0.302	−0.479	−0.486	0.710**	−0.490	−0.049	1

***Correlation is significant at the 0.01 level (two-tailed). *Correlation is significant at the 0.05 level (two-tailed).*

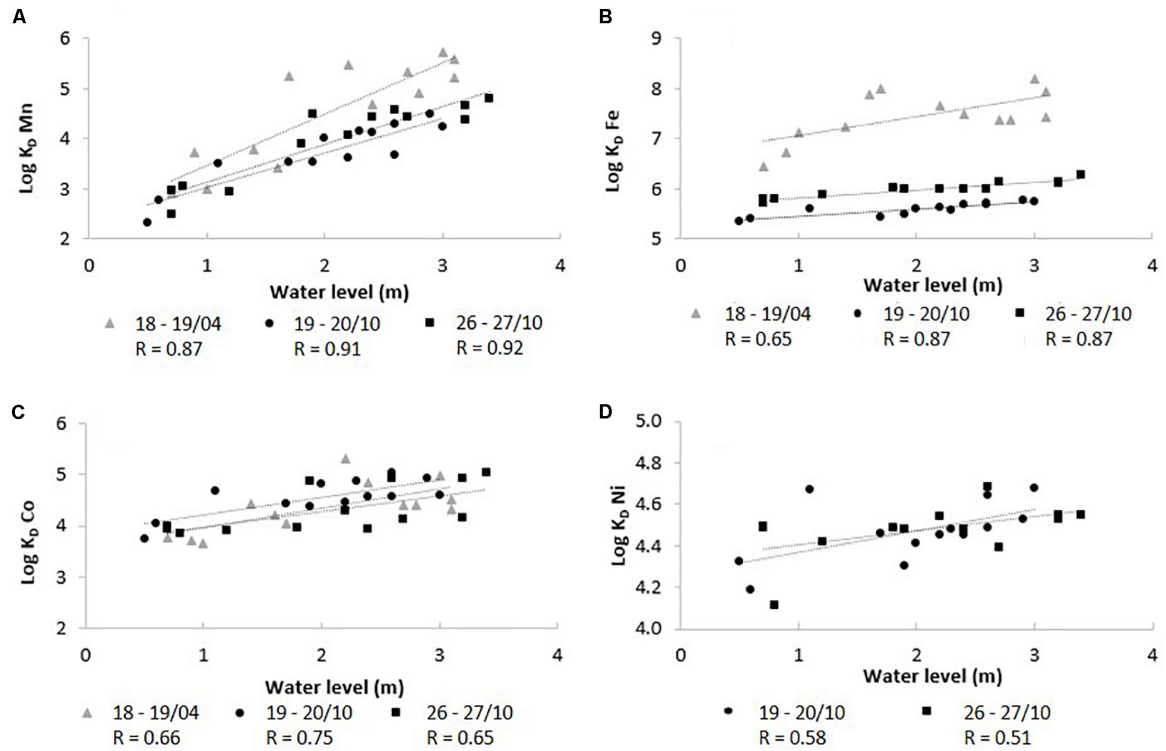

FIGURE 5 | Correlations between Log K_D of trace metals and water level for all tidal cycles in the creek during the dry (gray dots) and the wet seasons (black dots).

This hypothesis could be supported by the positive correlation between Log K_D^{Fe} and pH (r = 0.56 and 0.60 during the dry and the wet season, respectively, **Supplementary Figure S1**), and by the positive correlation between Log K_D^{Fe} and the water level confirming Fe precipitation with increasing pH. In addition, in the tidal creek, Log K_D^{Fe} ranged between 5.33 and 8.19 (**Figure 5B**), while in the Can Gio estuary, Log K_D^{Fe} varied between 6.39 and 7.6 (Thanh-Nho et al., 2018). Eventually, at low tide, TSS increase in the tidal creek, because of resuspension of bottom sediments due to the low water depth may also partly explain the higher Fe_P concentrations. However, the different dynamics between Fe and Mn in the creek evidenced that Fe_P distribution was not only related to physical processes, but that geochemical processes were involved, like Fe_D precipitation or colloidal flocculation. These results confirmed those obtained by Sanders et al. (2015), who suggested that small tidal estuaries may be important conduits for dissolved Fe to the ocean. However, we suggest that the great variability of pH and DO in mangrove ecosystems may limit this export under the dissolved form. Our results also confirm the hypothesis developed by Thanh-Nho et al. (2018) of Fe_P inputs from mangroves to the estuary, where they measured increased Fe_P concentrations at the "mangrove" station. In addition, like observed for different forms of carbon (Maher et al., 2013; Call et al., 2015), the type of tides and their ranges (i.e., neap and spring tides, respectively; **Figure 4**) influenced Fe concentrations in the tidal creek, being higher when a large tidal range (spring tides of 18-19/04/2015 and 26-27/10/2015, respectively) followed a small one (neap tide of 19-20/10/2015) because of elevated water residence time in the mangrove and larger mangrove area immerged.

Cobalt and Nickel Dynamics

Because of their similar distributions in dissolved and particulate phases in the mangrove tidal creek, Co and Ni are discussed together. Surprisingly, we did not observe any significant difference between Co_P and Ni_P concentrations at low tide and high tide. For similar salinity values in the estuary, Co_P concentrations ranged between 10 and 20 $\mu g\ L^{-1}$, and Ni_P between 40 and 50 $\mu g\ L^{-1}$ (Thanh-Nho et al., 2018), which was similar to what we measured in the tidal creek. We, thus, consider that estuarine waters were the main sources of Co_P and Ni_P in the tidal creek. However, the highest concentrations of Co_P and Ni_P were measured at the lowest water level of the spring tide during the wet season (**Figure 4**), which may suggest that these two elements were subject to the same geochemical processes than iron, being exported from mangrove soils under dissolved form and precipitating in the creek. This process may also explain the almost stable concentrations measured in the creek whatever the tidal period, without Co and Ni precipitations at low tide, a decrease of their concentrations would have been observed. In fact, Co_D and Ni_D presented higher concentrations in the creek water than the mouth of the Can Gio mangrove estuary irrespective of the season, with mean concentrations lower than 0.1 $\mu g\ L^{-1}$ for Co_D and lower than 1.0 $\mu g\ L^{-1}$ for Ni_D irrespective of the season (Thanh-Nho et al., 2018). We suggest that the increasing Co_D and Ni_D concentrations during

the ebb resulted from porewater inputs, being consistent with the negative correlations between Co_D, Ni_D and water levels during the tidal cycles ($r = -0.57$; -0.68 for Co_D during the dry and the wet season, **Supplementary Figure S1**; and $r = -0.59$ for Ni during the wet one, **Supplementary Figure S1**). However, we did not observe any good correlations between Co_D, Ni_D and ^{222}Rn (**Supplementary Figure S2**), most probably because, like we suggested, these elements were subject to geochemical processes during their transfer from the soil to the creek and also in the creek. Like for Mn_D, Co_D concentrations in the tidal creek were positively correlated to DOC ($r = 0.62$; 0.77 with DOC during the dry season and the wet season, respectively) (**Supplementary Figure S2**). Like Mn, in addition to a common origin, i.e., mangrove porewaters, we suggest the formation of organocobalt complexes, which may have increased the mobility of Co_D during its transfer from the porewater to the tidal creek (Noble et al., 2008). Log K_D^{Co} presented a large range of values, from 3.7 to 5.3, being positively correlated with the water level (**Figure 5C**). As a result of porewater inputs, Log K_D^{Co} decreased during the ebb. During the flood, Co_D may be adsorbed onto Fe-oxyhydroxide as they precipitate because of variable redox and pH conditions (Murray and Dillard, 1979). This hypothesis may be supported by the negative correlation between Co_D and pH ($r = -0.66$ and -0.72 during the dry and the wet season, respectively, **Supplementary Figure S1**) and by the negative correlation between Log K_D^{Co} and DOC ($r = -0.83$ during the dry season and $r = -0.58$ during the wet season, **Supplementary Figure S1**). Furthermore, the Co_D decrease during the flow can result from the physical mixing of the creek water with the estuarine water, containing lower Co_D concentrations.

Similarly to Co, Log K_D^{Ni} was positively correlated with the water level (**Figure 5D**), implying that physicochemical processes also played key roles in Ni partitioning in the tidal creek. During the flood, the decreasing Ni_D concentrations in the tidal creek most probably resulted from the dilution by the estuarine water, containing lower Ni_D, and/or from the adsorption onto TSS and the precipitation with Fe oxyhydroxide. The latter hypothesis may be supported by the negative correlation between Ni_D and pH ($r = -0.72$ during the wet season, **Supplementary Figure S1**). This result was consistent with the positive correlation between Log K_D^{Ni} and pH ($r = 0.65$, **Supplementary Figure S1**).

CONCLUSION

The present study evidences that trace metals dynamics in mangrove tidal creeks, that have no upstream inputs, depend both on the estuarine inputs during the flood, and mangrove soils inputs during the ebb. Mangrove soils can lose part of their trace metals stocks, exporting dissolved trace metals through process of porewater seepage. Additionally in the tidal creek, physical and geochemical processes during tidal cycles (i.e., physical dilution, precipitation, etc.) could modify trace metals partitioning between dissolved and particulate phases. Tidal ranges and irregularities of the tidal cycles influenced trace metal concentrations in the tidal creek, by controlling porewater seepage. When a larger area of mangrove is immerged and when there is an increased residence time of the water in the mangrove, like what happened when a strong tide followed a small one or during the rainy season, enhanced export of trace metals in the tidal creek during the ebb occurred. These processes resulted in large amount of dissolved Mn exported from the soils to the tidal creek and then possibly to the coastal ocean. Dissolved iron was also exported from mangrove soils, but conversely to Mn, we suggest that the different physico-chemical characteristics between the soils and the creek, notably higher dissolved oxygen concentrations and higher pH, resulted in its precipitation. Consequently, Fe was mainly exported from the creek to adjacent systems under particulate forms. Nickel and Cobalt dynamics were similar to the one of iron. Consequently, the mangrove ability to act as a sink for trace metals may be questioned and budget studies must be developed.

DATA AVAILABILITY STATEMENT

All datasets generated for this study are included in the article/**Supplementary Material**.

AUTHOR CONTRIBUTIONS

CM, NT-N, and T-TN-T performed the experimental design. NT-N, CM, TV, PT, and NC-H performed the data collection and statistical analyses. CM, NT-N, ES, and T-TN-T performed the data interpretation. All authors wrote the manuscript.

FUNDING

The research was funded by IRD (Institut de Recherche pour le Développement) through the BEST grant to NT-N. This research was supported by Vietnam National Foundation for Science and Technology Development (NAFOSTED) under grant number 05/2020/STS01.

ACKNOWLEDGMENTS

We would like to thank the authorities of Can Gio District People Committee and the CGMBR who facilitated the fieldwork.

SUPPLEMENTARY MATERIAL

The Supplementary Material for this article can be found online at: https://www.frontiersin.org/articles/10.3389/fenvs.2020.00139/full#supplementary-material

FIGURE S1 | Correlations between dissolved, particulate metal concentrations, physicochemical parameters, and water level over tidal cycles. The relationships between Log K_D of trace metals and physicochemical parameters are also presented.

FIGURE S2 | Correlations between trace metals and ^{222}Rn during the ebb in in the dry season (gray dots) and the wet season (black dots): **(a)** Mn_D, **(b)** Fe_D, **(c)** Co_D, **(d)** Ni_D and $_{222}Rn$; **(e)** DOC and ^{222}Rn, **(f)** Mn_D and DOC, **(g)** Co_D and Mn_D, **(h)** Co_D and DOC.

REFERENCES

Blasco, F., Aizpuru, M., and Gers, C. (2001). Depletion of the mangroves of Continental Asia. *Wetlands Ecol. Manag.* 9, 245–256.

Bouillon, S., Borges, A. V., Castañeda-Moya, E., Diele, K., Dittmar, T., Duke, N. C., et al. (2008). Mangrove production and carbon sinks: a revision of global budget estimates. *Glob. Biogeochem. Cycles* 22:GB2013.

Burnett, W., Kim, G., and Lane-Smith, D. (2001). A continuous monitor for assessment of 222Rn in the coastal ocean. *J. Radioanal. Nuclear Chem.* 249, 167–172.

Call, M., Maher, D. T., Santos, I. R., Ruiz-Halpern, S., Mangion, P., Sanders, C. J., et al. (2015). Spatial and temporal variability of carbon dioxide and methane fluxes over semi-diurnal and spring–neap–spring timescales in a mangrove creek. *Geochim. Cosmochim. Acta* 150, 211–225. doi: 10.1016/j.gca.2014.11.023

Clark, M. W., McConchie, D., Lewis, D. W., and Saenger, P. (1998). Redox stratification and heavy metal partitioning in Avicennia-dominated mangrove sediments: a geochemical model. *Chem. Geol.* 149, 147–171. doi: 10.1016/s0009-2541(98)00034-5

Dang, D. H., Lenoble, V., Durrieu, G., Omanovic, D., Mullot, J. U., Mounier, S., et al. (2015). Seasonal variations of coastal sedimentary trace metals cycling: insight on the effect of manganese and iron (oxy)hydroxides, sulphide and organic matter. *Mar. Pollut. Bull.* 92, 113–124. doi: 10.1016/j.marpolbul.2014.12.048

David, F., Marchand, C., Taillardat, P., Thành-Nho, N., and Meziane, T. (2018). Nutritional composition of suspended particulate matter in a tropical mangrove creek during a tidal cycle (Can Gio, Vietnam). *Estuar. Coast. Shelf Sci.* 200, 126–130. doi: 10.1016/j.ecss.2017.10.017

Deborde, J., Marchand, C., Molnar, N., Patrona, L., and Meziane, T. (2015). Concentrations and fractionation of carbon, iron, sulfur, nitrogen and phosphorus in mangrove sediments along an intertidal gradient (Semi-Arid Climate, New Caledonia). *J. Mar. Sci. Eng.* 3, 52–72. doi: 10.3390/jmse3010052

Dittmar, T., and Lara, R. J. (2001). Driving forces behind nutrient and organic matter dynamics in a mangrove tidal creek in North Brazil. *Estuar. Coast. Shelf Sci.* 52, 249–259. doi: 10.1006/ecss.2000.0743

Egawa, T., and Ooba, Y. (1963). Mineralogical studies of some soils in the central highland of Vietnam. *Soil Sci. Plant Nutr.* 9, 14–20. doi: 10.1080/00380768.1963.10431057

Fang, T. H., and Lin, C. L. (2002). Dissolved and particulate trace metals and their partitioning in a hypoxic estuary: the tanshui estuary in Northern Taiwan. *Estuaries* 25, 598–607. doi: 10.1007/bf02804893

Ferreira, T. O., Otero, X. L., Vidal-Torrado, P., and Macías, F. (2007). Effects of bioturbation by root and crab activity on iron and sulfur biogeochemistry in mangrove substrate. *Geoderma* 142, 36–46. doi: 10.1016/j.geoderma.2007.07.010

Furukawa, K., Wolanski, E., and Mueller, H. (1997). Currents and sediment transport in mangrove forests, estuarine, coastal and shelf. *Estuar. Coast. Shelf Sci.* 44, 301–310. doi: 10.1006/ecss.1996.0120

Hatje, V., Payne, T. E., Hill, D. M., McOrist, G., Birch, G. F., and Szymczak, R. (2003). Kinetics of trace element uptake and release by particles in estuarine waters: effects of pH, salinity, and particle loading. *Environ. Int.* 29, 619–629. doi: 10.1016/s0160-4120(03)00049-7

Holloway, C. J., Santos, I. R., Tait, D. R., Sanders, C. J., Rose, A. L., Schnetger, B., et al. (2016). Manganese and iron release from mangrove porewaters: a significant component of oceanic budgets? *Mar. Chem.* 184, 43–52. doi: 10.1016/j.marchem.2016.05.013

Kaly, U. L., Eugelink, G., and Robertson, A. I. (1997). Soil conditions in damaged North Queensland mangroves. *Estuaries* 20, 291–300.

Kristensen, E., Connolly, R. M., Otero, X. L., Marchand, C., Ferreira, T. O., and Rivera-Monroy, V. H. (2017). *Biogeochemical Cycles: Global Approaches and Perspectives. Mangrove Ecosystems: A Global Biogeographic Perspective*. Cham: Springer, 163–209.

Kuenzer, C., and Tuan, V. Q. (2013). Assessing the ecosystem services value of can gio mangrove biosphere reserve: combining earth-observation- and household-survey-based analyses. *Appl. Geogr.* 45, 167–184. doi: 10.1016/j.apgeog.2013.08.012

Lacerda, L. D., Martinelli, L. A., Rezende, C. A., Mozetto, A. A., Ovalle, A. R. C., Victoria, R. I., et al. (1988). The fate of heavy metals in suspended matter in a mangrove creek during a tidal cycle. *Sci. Tot. Environ.* 75, 249–259.

Lacerda, L. D., Ribeiro, M. G. Jr., and Gueiros, B. B. (1999). Manganese dynamics in a mangrove mud flat tidal creek in SE Brazil. *Mangroves Salt Marshes* 3, 105–115.

Leopold, A., Marchand, C., Deborde, J., Chaduteau, C., and Allenbach, M. (2013). Influence of mangrove zonation on CO2 fluxes at the sediment–air interface (New Caledonia). *Geoderma* 202-203, 62–70. doi: 10.1016/j.geoderma.2013.03.008

Luong, N. V., Tateishi, R., and Hoan, N. T. (2015). Analysis of an impact of succession in mangrove forest association using remote sensing and GIS technology. *J. Geogr. Geol.* 7:106.

Maher, D. T., Santos, I. R., Golsby-Smith, L., Gleeson, J., and Eyre, B. D. (2013). Groundwater-derived dissolved inorganic and organic carbon exports from a mangrove tidal creek: the missing mangrove carbon sink? *Limnol. Oceanogr.* 58, 475–488. doi: 10.4319/lo.2013.58.2.0475

Marchand, C., Albéric, P., Lallier-Vergès, E., and Baltzer, F. (2006). Distribution and characteristics of dissolved organic matter in mangrove sediment pore waters along the coastline of French Guiana. *Biogeochemistry* 81, 59–75. doi: 10.1007/s10533-006-9030-x

Marchand, C., Baltzer, F., Lallier-Vergès, E., and Albéric, P. (2004). Pore-water chemistry in mangrove sediments: relationship with species composition and developmental stages (French Guiana). *Mar. Geol.* 208, 361–381. doi: 10.1016/j.margeo.2004.04.015

Marchand, C., Fernandez, J. M., and Moreton, B. (2016). Trace metal geochemistry in mangrove sediments and their transfer to mangrove plants (New Caledonia). *Sci. Tot. Environ.* 562, 216–227. doi: 10.1016/j.scitotenv.2016.03.206

Marchand, C., Fernandez, J. M., Moreton, B., Landi, L., Lallier-Vergès, E., and Baltzer, F. (2012). The partitioning of transitional metals (Fe, Mn, Ni, Cr) in mangrove sediments downstream of a ferralitized ultramafic watershed (New Caledonia). *Chem. Geol.* 300-301, 70–80. doi: 10.1016/j.chemgeo.2012.01.018

Marchand, C., Lallier-Vergès, E., and Allenbach, M. (2011). Redox conditions and heavy metals distribution in mangrove forests receiving effluents from shrimp farms (Teremba Bay, New Caledonia). *J. Soils Sediments* 11, 529–541. doi: 10.1007/s11368-010-0330-3

McKee, K. L. (1993). Soil physicochemical patterns and mangrove species distribution-reciprocal effects. *J. Ecol.* 81, 477–487.

Murray, J. W., and Dillard, J. G. (1979). The oxidation of cobalt (II) adsorbed on manganese dioxide. *Geochim. Cosmochim. Acta* 43, 781–787. doi: 10.1016/0016-7037(79)90261-8

Noble, A. E., Saito, M. A., Maiti, K., and Benitez-Nelson, C. R. (2008). Cobalt, manganese, and iron near the Hawaiian Islands: a potential concentrating mechanism for cobalt within a cyclonic eddy and implications for the hybrid-type trace metals. *Deep Sea Res. Part II Top. Stud. Oceanogr.* 55, 1473–1490. doi: 10.1016/j.dsr2.2008.02.010

Noël, V., Marchand, C., Juillot, F., Ona-Nguema, G., Viollier, E., Marakovic, G., et al. (2014). EXAFS analysis of iron cycling in mangrove sediments downstream a lateritized ultramafic watershed (Vavouto Bay, New Caledonia). *Geochim. Cosmochim. Acta* 136, 211–228. doi: 10.1016/j.gca.2014.03.019

Noël, V., Morin, G., Juillot, F., Marchand, C., Brest, J., Bargar, J. R., et al. (2015). Ni cycling in mangrove sediments from New Caledonia. *Geochim. Cosmochim. Acta* 169, 82–98. doi: 10.1016/j.gca.2015.07.024

Patrick, W. H., and Jugsujinda, A. (1992). Sequential reduction and oxidation of inorganic nitrogen, manganese and iron in flooded soil. *Soil Sci. Soc. Am. J.* 56, 1071–1073. doi: 10.2136/sssaj1992.03615995005600040011x

Sadat-Noori, M., and Glamore, W. (2019). Porewater exchange drives trace metal, dissolved organic carbon and total dissolved nitrogen export from a temperate mangrove wetland. *J. Environ. Manag.* 248:109264. doi: 10.1016/j.jenvman.2019.109264

Sanders, C. J., Santos, I. R., Maher, D. T., Sadat-Noori, M., Schnetger, B., and Brumsack, H.-J. (2015). Dissolved iron exports from an estuary surrounded by coastal wetlands: can small estuaries be a significant source of Fe to the ocean? *Mar. Chem.* 176, 75–82. doi: 10.1016/j.marchem.2015.07.009

Strady, E., Blanc, G., Schäfer, J., Coynel, A., and Dabrin, A. (2009). Dissolved uranium, vanadium and molybdenum behaviours during contrasting freshwater discharges in the Gironde Estuary (SW France). *Estuar. Coast. Shelf Sci.* 83, 550–560. doi: 10.1016/j.ecss.2009.05.006

Taillardat, P., Pim, W., Marchand, C., Friess, D., Widory, D., Baudron, P., et al. (2018a). Porewater discharge and carbon fluxes in a mangrove tidal creek: the importance of in situ processes over tidal export. *J. Hydrol.* 563, 303–318. doi: 10.1016/j.jhydrol.2018.05.042

Taillardat, P., Ziegler, A. D., Friess, D. A., Widory, D., Truong Van, V., David, F., et al. (2018b). Carbon dynamics and inconstant porewater input in a mangrove tidal creek over contrasting seasons and tidal amplitudes. *Geochim. Cosmochim. Acta* 237, 32–48. doi: 10.1016/j.gca.2018.06.012

Taillardat, P., Ziegler Alan, D., Friess Daniel, A., Widory, D., David, F., Nobuhito, O., et al. (2019). Assessing nutrient dynamics in mangrove porewater and adjacent tidal creek using nitrate dual-stable isotopes: a new approach to challenge the outwelling hypothesis? *Mar. Chem.* 214:103662. doi: 10.1016/j.marchem.2019.103662

Tait, D. R., Maher, D. T., Macklin, P. A., and Santos, I. R. (2016). Mangrove pore water exchange across a latitudinal gradient. *Geophys. Res. Lett.* 43, 3334–3341. doi: 10.1002/2016gl068289

Tam, N. F. Y., and Wong, Y. S. (1999). Mangrove soils in removing pollutants from municipal wastewater of different salinities. *J. Environ. Qual.* 28, 556–564. doi: 10.2134/jeq1999.00472425002800020021x

Thanh-Nho, N., Marchand, C., Strady, E., Huu-Phat, N., and Nhu-Trang, T.-T. (2019a). Bioaccumulation of some trace elements in tropical mangrove plants and snails (Can Gio, Vietnam). *Environ. Pollut.* 248, 635–645. doi: 10.1016/j.envpol.2019.02.041

Thanh-Nho, N., Marchand, C., Strady, E., Vinh, T.-V., and Nhu-Trang, T.-T. (2019b). Metals geochemistry and ecological risk assessment in a tropical mangrove (Can Gio, Vietnam). *Chemosphere* 219, 365–382. doi: 10.1016/j.chemosphere.2018.11.163

Thanh-Nho, N., Strady, E., Nhu-Trang, T. T., David, F., and Marchand, C. (2018). Trace metals partitioning between particulate and dissolved phases along a tropical mangrove estuary (Can Gio, Vietnam). *Chemosphere* 196, 311–322. doi: 10.1016/j.chemosphere.2017.12.189

Turner, A., Millward, G., Bale, A., and Morris, A. (1993). Application of the KD concept to the study of trace metal removal and desorption during estuarine mixing. *Estuar. Coast. Shelf Sci.* 36, 1–13. doi: 10.1006/ecss.1993.1001

USEPA (2007). *US Environmental Protection Agency, Method 3051A: Microwave Assisted Acid Digestion of Sediments, Sludges, Soils, and Oils, part of Test Methods for Evaluating Solid Waste*. Washington, DC: USEPA.

Van Ryssen, R., Alam, M., Goeyens, L., and Baeyens, W. (1998). The use of flux-corer experiments in the determination of heavy metal re-distribution in and of potential leaching from the sediments. *Water Sci. Technol.* 37, 283–290. doi: 10.2166/wst.1998.0763

Vinh, T. V., Allenbach, M., Aimée, J., and Marchand, C. (2019). Seasonal variability of CO2 fluxes at different interfaces and vertical CO2 concentrations profiles in a *Rhizophora* mangrove stand (Can Gio, Viet Nam). *Atmos. Environ.* 201, 301–309. doi: 10.1016/j.atmosenv.2018.12.049

Vinh, T. V., Allenbach, M., Linh, K. T. V., and Marchand, C. (2020). Changes in leaf litter quality during its decomposition in a tropical planted mangrove forest (Can Gio, Vietnam). *Front. Environ. Sci.* 8:10. doi: 10.3389/fenvs.2020.00010

Wolanski, E. (1995). Transport of sediment in mangrove swamps. *Hydrobiologia* 295, 31–42. doi: 10.1007/978-94-011-0289-6_5

Xiao, R., Bai, J., Lu, Q., Zhao, Q., Gao, Z., Wen, X., et al. (2015). Fractionation, transfer, and ecological risks of heavy metals in riparian and ditch wetlands across a 100-year chronosequence of reclamation in an estuary of China. *Sci. Total Environ.* 517, 66–75. doi: 10.1016/j.scitotenv.2015.02.052

Conflict of Interest: The authors declare that the research was conducted in the absence of any commercial or financial relationships that could be construed as a potential conflict of interest.